The Role of Relativity in Magnetism: Calculating Magnetic Moments in Solids

By

Kevin P. Driver

Submitted to the Graduate School

in partial fulfillment of the requirements

for the Doctoral Candidacy Examination

Department of Physics

The Ohio State University

2006

Contents

I. Introduction 3

II. Background: Relativity Begets Magnetism 4

A. Relativity in Quantum Systems 4

B. Fundamentals of Magnetism 6

III. Methodology: DFT and Neutron Scattering 10

A. Relativistic Electronic Structure 10

B. Experimental Measurement of Magnetic Moments 18

IV. Results: Magnetic Moments in Solids 20

A. 3d Transition Metals: ($V_{CF} \gg V_{SO}$) 20

B. Lanthanides: ($V_{CF} \ll V_{SO}$) 22

C. Actinides: ($V_{CF} \simeq V_{SO}$) 25

V. Conclusion 29

Acknowledgments 30

References 30

I. INTRODUCTION

Since the development of Quantum Mechanics, much progress has been made towards understanding the microscopic origin of magnetism in solids. However, a completely coherent model of magnetism in solids is still missing. Partly, this is due to the fact that magnetism is a complex many-body problem with its roots in relativistic quantum field theory. At a basic level, magnetism comes from spin and orbital properties of electrons. These electrons can be localized in orbitals or itinerant in conduction bands. The itinerant behavior is exemplified by 3d transition metals, while the localized behavior is seen in 4f, lanthanide systems. Both types of magnetism show up in the 5f, actinide systems. There have been many approximate Hubbard- and Stoner-type models which approach magnetism from either the localized or itinerant perspective. Although, a complete model of magnetism should be able to cope with both aspects of magnetism.

A recent attempt at a more complete description of magnetism involves a relativistic band structure theory that has been developed within the framework of Density Functional Theory (DFT). In this paper, the cornerstones of this relativistic DFT approach will be sketched as well as simplification and correction methods for practical calculations. Studies of magnetic moments in characteristic 3d, 4f, and 5f solids using this method are discussed and compared with experimental measurements. The paper is organized as folows: In section II, the importance of relativity in magnetism addressed. Section III focuses on the DFT method used to compute magnetic moments and how these moments can be measured with neutron scattering. Section IV compares calculated magnetic moments in 3d, 4f, and 5f solids with experimental measurements. Finally, conclusions are drawn in Section V.

II. BACKGROUND: RELATIVITY BEGETS MAGNETISM

A. Relativity in Quantum Systems

Non-relativistic quantum mechanics, described by Schrödinger's wave equation, is very successful for problems in which the velocity of the electron is small compared with the speed of light. However, Schrödinger's equation cannot account naturally for fine structure corrections of order $(v/c)^4$, namely relativistic mass increase and spin-orbit coupling. The relativistic mass increase is especially important in heavy atom systems because one knows from Bohr's model that speed scales with atomic number, Z. Furthermore, spin, which is a fundamental property of the electron and particularly important in magnetism, is not built into Schrödinger's equation. A proper equation for the electron should naturally incorporate relativistic effects and spin.

Such a relativistic description of quantum mechanics is found in the Dirac equation (here, coupled to the potential $(\mathbf{A}, V)$):

$$i\hbar\frac{\partial\Psi}{\partial t} = (c\alpha\cdot(\mathbf{p} - \frac{q\mathbf{A}}{c}) + \beta mc^2 + qV)\Psi, \tag{1}$$

where $\mathbf{p}$ is the momentum operator, A is a vector potential, V is a scalar potential, and α and β are the 4×4 *Dirac Matrices*,

$$\alpha = \begin{pmatrix} 0 & \sigma \\ \sigma & 0 \end{pmatrix} \quad \text{and} \quad \beta = \begin{pmatrix} I & 0 \\ 0 & -I \end{pmatrix}.$$

Here, σ are the Pauli matrices and I is the 2x2 identity matrix. Of course, the wave functions

are four-component column vectors written as

$$\Psi = \begin{pmatrix} \Phi \\ \\ \chi \end{pmatrix},$$

where Φ and χ are two component spinors [1, 2].

The Dirac equation not only takes the relativistic kinetic energy of the electron into account, but spin and fine structure corrections come out naturally also. It follows that, in a strict sense, spin and spin-orbit effects, which are certainly important in magnetism, are relativistic effects. One can see this explicitly by splitting the Dirac equation into two coupled equations in Φ and χ, setting $\mathbf{A} = 0$, and assuming V is spherically symmetric. To order $(v/c)^4$, one gets the following equation for Φ: $H\Phi = E\Phi$, where

$$H = \frac{p^2}{2m} + V(r) - mc^2\left(\frac{1}{8}\left(\frac{p}{mc}\right)^4\right) + \frac{1}{2m^2c^2}\frac{1}{r}\frac{dV}{dr}(\mathbf{S}\cdot\mathbf{L}) - \frac{\hbar^2}{4m^2c^2}\frac{dV}{dr}\frac{\partial}{\partial r} \qquad (2)$$

The first and second term comprise the non-relativistic Schrödinger equation. The third term is the relativistic correction to the kinetic energy (or mass). The fourth term corresponds to spin-orbit coupling, and the last term is the so-called Darwin correction. The Darwin term can be thought of as a relativistic correction to the potential [1, 3].

Some physical consequences of the mass correction term (sometimes called the scalar term) are the contraction of s and p electron orbitals in atoms. The s and p electrons have a large probability density near the nucleus and, thus, tend to move at speeds near c. In what is known as a *direct* relativistic effect, the corresponding mass increase contracts the orbitals. As a consequence, the d and f orbitals will expand a little due to shielding effects.

That is, they undergo *indirect* relativistic effects. [4].

Of course, in this paper, the main interest is what role all of these relativistic effects play in determining the magnetic moment of an atom. The origin of magnetism resides with the fact that electrons have spin and they orbit about the nucleus of an atom. Spin and orbital magnetic moments,

$$\mu_{\mathbf{spin}} = -2(\frac{e}{2m})\mathbf{S} \quad \text{and} \quad \mu_{\mathbf{orb}} = -(\frac{e}{2m})\mathbf{L}, \tag{3}$$

combine to produce a net atomic moment. Furthermore, the spin moment of an electron interacts with the magnetic field it feels as it orbits through the electric field of the nucleus. This is the spin-orbit effect. The next section discusses how one goes about organizing these properties, which must obey certain physical rules to produce a magnetic material.

B. Fundamentals of Magnetism

On a microscopic level, magnetic properties of a solid are derived from the ground state properties of incompletely filled electron shells. The magnetic response observed in a particular system largely depends on how the spin and orbital properties of these electrons end up combining after obeying Pauli's exclusion principle and minimizing Coulomb repulsion [5–9]. This fact is made evident in Hund's three rules for determining the ground state (lowest energy) electronic configuration of an *atom*:

1) *Spin Polarization*: Arrange electrons to maximize total spin, **S**, obeying Pauli's exclusion principle. In effect, this is minimizing Coulomb energy while not allowing two parallel spins to occupy the same state. The energy decrease due to the preference for parallel spins is called the *exchange energy*.

2) *Orbital Polarization*: Arrange the electrons to maximize the total orbital angular momentum, **L**, consistent with the exclusion principle and the first rule. This, again, is effectively a scheme to minimize Coulomb repulsion. In a classical picture, one can imagine that by having the electrons orbit in the same direction, they can avoid encountering each other more effectively.

3) The total angular momentum, **J** is found using $J = |L - S|$ for less than half filled shells and $J = |L+S|$ for more than half filled shells. This rule is an attempt to minimize spin-orbit interaction energy.

In solids, depending on whether the crystal is insulating or conducting, magnetism has historically been approached from two different schools of thinking: either a localized or itinerant point of view. In the localized concept of magnetism, the electrons and their magnetic properties remain associated with their respective paramagnetic ion in a insulating crystal. Conversely, in the itinerant picture, the conduction electrons are responsible for magnetism. Consider the nature of these two models in more detail:

In insulators, paramagnetic ions with unpaired electrons exhibit permanent dipole moments due to the net angular momentum, $\mathbf{J} = \mathbf{L} + \mathbf{S}$, of the ion. Different types of magnetic ordering may arise based on the specific alignment of the atomic magnetic moments, favored by atomic exchange interactions. Strictly speaking, a crystal does not have to be an insulator to exhibit localized magnetism. As in the case of the rare-earth metals, the unfilled 4f orbital is localized to such an extent that it does not form conduction bands in a solid. In either case, Hund's rules for the free ion can be used to determine **J**, **L**, and **S** for each

atom. Then, the magnetic moment of each atom is given by

$$\mu_{atom} = g_J \mu_B |\mathbf{J}| = g_J \mu_B [J(J+1)]^{1/2} \tag{4}$$

where g_J is the Landé g factor, given by: $g_J = 1 + \frac{J(J+1)-L(L+1)+S(S+1)}{2J(J+1)}$.

Whereas localized magnetism is characterized by insulating states, itinerant magnetism is associated with metallic behavior. In the itinerant case, the unfilled orbitals broaden into (narrow) bands by overlapping with neighboring orbitals. There is an interaction between the nearly free conducting electrons and the localized electrons that produces a resultant magnetic state. Magnetic ordering in this situation refers to the redistribution of conducting electrons with spin up and spin down electrons in separate bands.

For example, spontaneous ferromagnetism observed in transition metals Fe, Co, and Ni, is not possible to understand on the basis of localized moments on atoms. Normally, in a metal, there are an equal number of spin-up and spin-down electrons filling up states to the Fermi energy. A stable ferromagnetic state in the absence of an external field can only arise if there is a spontaneous splitting of the spin population in the bands (i.e. spin polarization). This can happen if it is energetically favorable for the system as a whole to promote electrons above the the Fermi level and reverse their spin. That is, when the exchange energy gained is greater than the cost in energy to promote and reverse the spin of electrons above the Fermi level, a stable ferromagnetic state will form. In practice, this only happens for systems in which Coulomb effects are strong and also have narrow bands with a high density of states at the Fermi surface. Of the 3d transition metals, only Fe, Co, and Ni have sufficient exchange energy gain to retain a ferromagnetic state.

In addition to the physics underlying Hund's rules, other external effects may influence the electronic and magnetic behavior in a solid. One important effect that tends to override the intuition of Hund's rules is crystal field splitting. In general, the magnitude of the crystal field effect on a system will depend on the symmetry of the crystal and the distance between ions. Crystal fields have the most effect on systems in which orbitals extend out far enough from the nucleus to have significant overlap with orbitals on neighboring atoms, such as in 3d transition metals. It is well known that crystal fields largely quench the orbital angular momentum in the 3d transition metals. Thus, the orbital magnetic moment in the 3d transition metals is expected to be significantly reduced. However, for 4f orbitals, crystal field effects are expected to be much less noticeable because they are less spatially extended and they are shielded by other filled orbitals.

It is difficult to find a theory that takes the accumulation of all these underlying effects into account to calculate magnetic moments and get agreement with experimental measurements. In order to get accurate results, one can not ignore the effect of Coulomb interactions between electrons (correlation effects) and the effects of exchange on the motions of electrons. It is necessary to use the formalism of electronic structure calculations that include the effects of spin polarization and exchange-correlation. A useful approach that will be focused on in this paper is *relativistic (spin)-density functional theory* (DFT) used with the *local spin-density approximation* (LSDA) for exchange-correlation effects. The rough message of Hund's rules will still be prevalent, and corrections to LSDA must be added to account for all of Hund's rules. The details of this methodology are the subject of the next section.

III. METHODOLOGY: DFT AND NEUTRON SCATTERING

A. Relativistic Electronic Structure

In calculating properties of systems that are inherently relativistic, one would like there to exist a relativistic successor to the many-body Schrödinger equation. Unfortunately, no closed-form, relativistic many-body equation is known, and one is forced to resort to approximate schemes right away [10, 11]. The most accurate choice one can make is to use the Dirac Hamiltonian for the one-body terms, with the Coulomb repulsion serving as the two-body interaction, resulting in the Dirac-Coulomb equation. In quantum chemistry, one often employs one-electron solutions to this equation through the self-consistent field procedure, yielding a Dirac-Hartree Fock scheme [12, 13]. These equations work well for atoms and small molecules, but are too computationally expensive for real solid simulations. The method of choice for solids is a relativistic formulation of Density Functional Theory (DFT), where properties are determined by the electron density. In practice, as will be discussed, one even avoids solving a fully relativistic DFT, tossing out any terms involving angular momentum, and employing corrections to capture the missing relativistic effects. In this section, non-relativistic DFT is reviewed and extended to relativistic form, and then a more practical spin-polarized DFT is discussed along with the appropriate relativistic corrections for magnetism.

Non-relativistic DFT has been used very successfully in many cases for simulating real solids. It allows for a great simplification in solving the many-body problem, $H\Psi = E\Psi$. The framework of the theory consists of two major parts:

The first part is a theorem developed by Hohenberg and Kohn [14] which says that the

total energy, E_{tot}, of a system is a unique functional of the electron density, $n(\mathbf{r})$. Furthermore, the functional $E_{tot}[n(\mathbf{r})]$ is minimized for the ground state density, $n_{GS}(\mathbf{r})$. In short, this affords the possibility of calculating electronic properties based on the electron density (3 spatial variables), instead of the 3N-variable many-body wave function.

The second part of the theory involves the construction and variational minimization of the total energy functional, $E_{tot}[n(\mathbf{r})]$, with respect to variations in the electron density. This part of the theory, developed by Kohn and Sham [15] states that the many-body Schrödinger equation can be mapped onto the problem of solving an effective single-particle wave equation with an effective potential, V_{eff}. The first step is to write the total energy functional as

$$E_{tot}[n(\mathbf{r})] = T[n(\mathbf{r})] + E_{e-e}[n(\mathbf{r})] + E_{xc}[n(\mathbf{r})] + \int V_{ext}(\mathbf{r})n(\mathbf{r})d\mathbf{r} \tag{5}$$

where T is the kinetic energy of a noninteracting system, E_{e-e} is the electron-electron interaction energy, E_{xc} is the exchange-correlation energy, and V_{ext} represents an external potential including the ions. By minimizing this total energy functional with respect to variations in the electron density, subject to the constraint that the number of electrons are fixed, an effective one-particle equation is obtained:

$$\left\{-\frac{\hbar^2}{2m}\nabla^2 + V_{eff}[n(\mathbf{r})]\right\}\psi_i(\mathbf{r}) = \epsilon_i\psi_i(\mathbf{r}), \tag{6}$$

where V_{eff} is an effective potential given by

$$V_{eff}[n(\mathbf{r})] = V_{ext}[n(\mathbf{r})] + V_{e-e}[n(\mathbf{r})] + \frac{\delta E_{xc}[n(\mathbf{r})]}{\delta n(\mathbf{r})}. \tag{7}$$

Eqs. (6) and (7), are known as the Kohn-Sham equations. The quantities $\psi_{\rm i}$ and ϵ_i are auxiliary quantities used to calculate the electron density and total energy, not the wave function and energy of real electrons. The only unknown is the is the exchange-correlation potential. In the most common approximation, known as the Local Density Approximation (LDA), the exchange-correlation energy is calculated using quantum Monte Carlo results of the homogeneous, interacting electron gas [16]:

$$E_{xc}^{LDA}[n(\mathbf{r})] = \int n(\mathbf{r})\epsilon_{xc}^{heg}[n]d\mathbf{r}, \tag{8}$$

where $\epsilon_{xc}^{heg}[n]$ is the exchange and correlation energy per particle in the homogeneous electron gas [17].

The Kohn-Sham equations are then solved self-consistently. One starts by assuming a charge density $\mathrm{n}(\mathbf{r})$, calculates $\mathrm{V_{xc}}[\mathrm{n}(\mathbf{r})]$, and then solves Eq. (6) for the wave functions, $\psi_{\rm i}(\mathbf{r})$, using a standard band theory technique. From the wave functions obtained, one calculates a new charge density:

$$n(\mathbf{r}) = \sum_{i}^{occ.} \left|\psi_i(\mathbf{r})\right|^2. \tag{9}$$

This procedure is then repeated until the charge density is converged.

In fully relativistic DFT [16, 18–22], the density, $n(\mathbf{r})$, is substituted by the four-vector analogue, the four-current, $J_\mu(\mathbf{r}) = [n(\mathbf{r}), \mathbf{J}(\mathbf{r})]$ and the potentials $V_{ext}(\mathbf{r})$ by the four-potential, $A_\mu^{ext}(\mathbf{r}) = [V(\mathbf{r}), \mathbf{A}(\mathbf{r})]$. The formalism then proceeds exactly as it did in non-relativistic DFT:

Analogous with the above discussion, the *relativistic Hohenberg-Kohn theorem* says that

the ground state energy is a unique functional of the four-current density, $J_\mu(\mathbf{r})$, and that the minimum of this functional, $\mathrm{E}^{\mathrm{rel}}_{\mathrm{tot}}[\mathrm{J}_\mu(\mathbf{r})]$ is the ground state energy. The energy functional is again divided up into respective contributions:

$$E^{rel}_{tot}[J_\mu(\mathbf{r})] = T[J_\mu(\mathbf{r})] + E_{e-e}[J_\mu(\mathbf{r})] + E_{xc}[J_\mu(\mathbf{r})] + \int J^\mu(\mathbf{r}) A^{ext}_\mu(\mathbf{r}) d\mathbf{r} \tag{10}$$

In practice, relativistic DFT in this full form is never used to perform simulations of large systems, such as solids. The best one usually does for solids is to use a "spin-only" version [16, 18, 20, 23] (plus correction terms, discussed later), which goes by the name of *spin-polarized relativistic DFT*. In this scheme, the current density is decomposed nontrivally into orbital and spin parts [24] and all terms involving A^{ext} are dropped to yield the "spin-only" analogue of Eq. (10):

$$E^{SRDFT}_{tot}[J_\mu(\mathbf{r})] = T[J_\mu(\mathbf{r})] + E_{e-e}[J_\mu(\mathbf{r})] + E_{xc}[J_\mu(\mathbf{r})] + \int (n(\mathbf{r}) V_{ext}(\mathbf{r}) - \mathbf{m}(\mathbf{r}) \cdot \mathbf{B_{ext}}(\mathbf{r})) d\mathbf{r} \tag{11}$$

where $\mathbf{m}$ is the spin density and $\mathbf{B_{ext}}$ is a external magnetic field. Since the relativistic kinetic energy is included, but not the spin-orbit term, one often refers to this equation as being *scalar relativistic*. The non-relativistic version of this equation is just Eq. (5) with $\mu_B \mathbf{m} \cdot \mathbf{B_{ext}}$ added to potential, i.e spin-polarized DFT. Going through the Kohn-Sham minimization process, the total energy functional is minimized with respect to the variations in the four-current to yield a single particle equation (the "spin-only" Dirac-Kohn-Sham equation):

$$(c\alpha \cdot \mathbf{p} + \beta mc^2 + V_{eff}(\mathbf{r}) - \mathbf{m}(\mathbf{r}) \cdot \mathbf{B_{eff}}(\mathbf{r}))\psi_i(\mathbf{r}) = \epsilon_i \psi_i(\mathbf{r}) \tag{12}$$

with

$$V_{eff}[n(\mathbf{r})] = V_{ext}[n(\mathbf{r})] + V_{e-e}[n(\mathbf{r})] + \frac{\delta E_{xc}[n(\mathbf{r}), m(\mathbf{r})]}{\delta n(\mathbf{r})} \tag{13}$$

$$B_{eff}(\mathbf{r}) = B_{ext}(\mathbf{r}) - \frac{1}{\mu_B}\frac{\delta E_{xc}[n(\mathbf{r}), m(\mathbf{r})]}{\delta m(\mathbf{r})} \tag{14}$$

$$\mathbf{m}(\mathbf{r}) = \mu_B \sum_i^N \psi_i^\dagger(\mathbf{r})\beta\sigma\psi_i(\mathbf{r}) \tag{15}$$

$$n(\mathbf{r}) = \sum_i^{occ.} \psi_i^\dagger(\mathbf{r})\psi_i(\mathbf{r}). \tag{16}$$

These equations constitute a set of self-consistent equations for a "spin-only" magnetic system. That is, the magnetic field has been coupled to the spin of the electrons, but not their orbital motion. Eq. (12) looks very much like the single-particle Dirac equation (Eq. (1)), but ψ_i and ϵ_i are not single-particle energies and wave functions, they are auxiliary quantities used to form the four-current density and total energy. The exchange-correlation used most frequently is the spin analogue to LDA, namely the Local Spin Density Approximation (LSDA) [22, 25]:

$$E_{xc}^{LSDA}[n(\mathbf{r}), m(\mathbf{r})] = \int n(\mathbf{r})\epsilon_{xc}^{spheg}[n(\mathbf{r}), m(\mathbf{r})]d\mathbf{r}, \tag{17}$$

where $\epsilon_\mathrm{xc}^\mathrm{spheg}[\mathrm{n}, \mathrm{m}]$ is the exchange and correlation energy per particle in a spin-polarized, homogeneous (interacting) electron gas with charge density, n, and spin (magnetization) density, m. Note that, because LSDA is based on a electron gas, no orbital information is included in E_{xc}.

Consequently, if the external magnetic field is set to zero, magnetic solutions to Eq. (12) can still exist because of the derivative of E_{xc} with respect to the spin density, m, in Eq. (14) [16]. If such a solution turns out to be lower in energy than a non-magnetic solution,

then it is possible to predict a net (spontaneous) *spin polarization*. One can then calculate the magnetic spin moment from the spin magnetization [12, 22]:

$$\mu_{\mathbf{spin}} = \mu_B \int \mathbf{m}(\mathbf{r}) d\mathbf{r} \tag{18}$$

Thus, in some sense, Hund's first rule is built into the LSDA.

Before moving on to discuss corrections for Hund's second and third rules, it is necessary to make few general remarks about band theory methods [23, 26]. As mentioned above, there are a number of standard band structure methods one can choose to solve the single-particle equation (Eq. (12)). In all of these methods, the major issue is how one chooses to represent the Kohn-Sham orbitals, ψ_i. Nearly all the methods invoke some sort of basis set expansion: $\psi_i = \sum_\alpha c_{i\alpha}\phi_\alpha(\mathbf{r})$, where the $\phi_\alpha(\mathbf{r})$ are the basis functions and the $c_{i\alpha}$ are expansion coefficients. Once the basis is chosen, the coefficients become the only variables in the problem, and, since the total energy in DFT is variational, solving the Kohn-sham equation amounts to determining the coefficients (for occupied orbitals) that minimize the total energy. This is referred to as the *variational step*. Therefore, the eigenvalue equation, $H\psi = E\psi$, is rewritten as the characteristic matrix equation:

$$(\mathbf{H} - \epsilon_i \mathbf{S})c_i = \mathbf{0}, \tag{19}$$

where H is the Hamiltonian matrix ans S is the overlap matrix (with respective elements $\langle \phi_\alpha^* | H | \phi_\alpha \rangle$ and $\langle \phi_\alpha^* | \phi_\alpha \rangle$), ϵ_i are the electron eigenvalues, and the c_i are column vectors containing the basis expansion coefficients. Once the matrix equation is solved, the eigenvalues and eigenvectors can be used to calculate the partial density of states. Then new charge and

spin densities can be constructed as part of the self-consistent cycle.

Now, in most magnetic systems, one also needs to go beyond spin polarization and include orbital magnetic moments to get good agreement with experiment. Essentially, this means one needs to find a way to incorporate Hund's second and third rules on top of the LSDA scheme. A common method of doing this is to have two correction terms: one for orbital polarization (Hund's second rule) and one for spin-orbit coupling (Hund's third rule).

Accounting for orbital polarization in magnetic systems has largely been of the *ad hoc* nature. This isn't too surprising since there is no consistent many-body theory of orbital magnetism [27]. A popular *ad hoc* scheme has been developed by Brooks *et al.* [28, 29]. Their idea came from noting that Hund's first rule can be thought of as being due to a Hamiltonian of the form $-I\sum_{i\neq j}\mathbf{s_i}\cdot\mathbf{s_j}$. A mean field approach to this Hamiltonian yields an energy $E=-IS_z^2$, where I is a spin-exchange constant. In analogy, Brooks suggested that Hund's second rule corresponds to a Hamiltonian of the form $\frac{1}{2}\sum_{i\neq j}\mathbf{l_i}\cdot\mathbf{l_j}$. The mean field treatment leads to a orbital polarization term in the total energy functional expression: $E_{OP}=R\mathbf{L}^2$, where $\mathbf{L}$ is the total orbital angular momentum of the partially filled electron shell and R is a "orbital-exchange" coefficient, known as the Racah parameter. When proceeding through the Kohn-Sham minimization, this energy results in a shift of the one-electron eigenvalues of

$$\delta\epsilon_{m_l}=\frac{\partial E_{OP}}{\partial n_{ml}}=-RLm_l \tag{20}$$

for the state m_l. The spin-up and spin-down manifolds are split into equidistant levels, with the positive m_l states lower in energy than the negative m_l states. By tallying up the contributions to the total orbital angular momentum, one can calculate the orbital magnetic moment. Although, as will be discussed next, spin-orbit effects may also contribute to the

orbital moment.

Indeed, some magnetic systems cannot be described properly without Hund's third rule, which requires one to include spin-orbit coupling into the calculation [22, 30, 31]. It was shown that the spin-orbit interaction naturally comes out of the Dirac equation (Eq. (2)) :

$$H_{SO} = \frac{1}{2m^2c^2}\frac{1}{r}\frac{\partial V(r)}{\partial r}\mathbf{S}\cdot\mathbf{L} \tag{21}$$

In this form, it is obvious the spin and angular momentum are coupled. The main importance of this interaction in magnetic systems is that the coupling lifts the degeneracy between m_l and $-m_l$ states (from the S_zL_z term), thereby inducing a orbital moment. In hydrogenic atoms, the spin-orbit energy scales as Z^4, but is proportional to α^4, where α is the fine structure constant. This means the effect becomes increasingly important in heavier atoms, but is secondary in size to Coulomb effects ($\sim \alpha^2$). In the presence of crystal field quenching, spin-orbit coupling may be the dominant source of orbital magnetism.

One often avoids dealing with spin-orbit coupling in electronic structure calculations because when the interaction is turned on, spin and angular momentum are no longer good quantum numbers. One must work with eigenstates of the total angular momentum, which amounts to doubling the size of the basis required for solving the characteristic matrix equation. This drastically reduces the speed of the computation. Fortunately, a method has been developed to circumvent this problem, known as *second variational treatment* [23, 26]. The basic idea is to solve the scalar relativistic (SR) equation first (Eq. (12)) and get the set of corresponding coefficients and eigenvalues from Eq. (19). That is, solve

$$(\mathbf{H}^{SR} - \epsilon_N^{SR}\mathbf{S}^{SR})c_N^{SR} = \mathbf{0} \tag{22}$$

for N solutions, C_N^{SR} and ϵ_N^{SR}, which describe a pure spin basis. Then from those solutions, form a new basis for the total angular momentum and solve the matrix equation a second time using the Hamiltonian

$$\mathbf{H} = \epsilon^{SR}\delta_{ij} + \mathbf{H}^{SO}. \tag{23}$$

Note that H^{SR} and S^{SR} will be diagonal in this new basis. The main trick is, the second time, one only uses only the lowest n scalar relativistic orbitals as calculated in the first step. In general, one finds n can be much smaller than N.

In summary, the main idea of this section is to use spin-polarized, scalar relativistic DFT with the orbital polarization and spin-orbit corrections to calculate magnetic properties of materials. Effectively, this approach takes all three Hund's rules into account. In this paper, the scope is limited to examine how well this scheme does for the calculation of atomic magnetic moments in solids. Of course, to get a measure of computational accuracy, there must be reliable experiments with which to compare. The next section outlines a common experimental technique to measure magnetic moments.

B. Experimental Measurement of Magnetic Moments

Ultimately, to determine the accuracy of a computational method, one must check the results against experimental measurements. A common technique used to measure spin and orbital magnetic moments is *neutron magnetic scattering* [32–37]. The fact that neutrons are neutral in electric charge and have a magnetic moment makes them an ideal probe of atomic magnetic moments. Spin (μ_s) and orbital (μ_L) magnetic moments can be determined separately because they interact differently with the neutron magnetic moment.

In fact, the angular dependence through which the neutrons are scattered depends on the Fourier transform of the magnetization, i.e. the form factor [37]. The spin and orbital magnetizations, $M_S(\mathbf{r})$ and $M_L(\mathbf{r})$, respectively, are different so that one can write down two form factors [33]:

$$f_L(\mathbf{Q}) = \int M_L(\mathbf{r}) \exp(i(\mathbf{Q}) \cdot (\mathbf{r})) \quad \text{and} \quad f_S(\mathbf{Q}) = \int M_S(\mathbf{r}) \exp(i(\mathbf{Q}) \cdot (\mathbf{r})), \tag{24}$$

where $Q = 4\pi \sin\theta/\lambda$ is the scattering vector with θ being the scattering angle and λ being the wavelength of the neutron.

In general, one can expand the form factors in a series of Bessel function transforms [38], $< j_i >$, of single-electron radial probability distributions, $|\psi_i|^2$:

$$f(\mathbf{Q}) = \langle j_0 \rangle + C_2 \langle j_2 \rangle + C_4 \langle j_4 \rangle + \ldots, \tag{25}$$

where the Bessel transform is $\langle j_i(Q) \rangle = \int_0^\infty |\psi_i|^2 (r) j_i(Qr) dr$. Then, in the dipole (small Q) approximation [39], one can show $f_S \approx \langle j_0 \rangle$ and $f_L \approx \langle j_0 \rangle + \langle j_2 \rangle$. It follows that, since the total moment is $\mu_{tot} = \mu_L + \mu_S$, the total *magnetic amplitude*, which can be directly measured, is given by

$$\mu f(\mathbf{Q}) = \mu_S f_S(\mathbf{Q}) + \mu_L f_L(\mathbf{Q}) \tag{26}$$

$$= \mu_S \langle j_0 \rangle + \mu_L (\langle j_0 \rangle + \langle j_2 \rangle) = \mu_{tot} \left[\langle j_0 \rangle + C_2 \langle j_2 \rangle \right], \tag{27}$$

where $C_2 = \mu_L/\mu_{tot}$. Finally, using a least-squares analysis, one can fit Eq. (27) to the measured magnetic amplitudes and determine values of μ_{tot} and C_2. If follows that one can

extract μ_S and μ_L [35]. Moments measured in this way are compared with spin-polarized calculations in the next section.

IV. RESULTS: MAGNETIC MOMENTS IN SOLIDS

A. 3d Transition Metals: ($V_{CF} \gg V_{SO}$)

The 3d transition metals are known for their itinerant magnetic behavior, with Fe, Co, and Ni being the archetypal examples of itinerant ferromagnetism [40]. Spin polarization comes about when the 3d conduction electrons become spontaneously spin-split as described earlier. Fig. (1) shows that 3d orbitals are spatially localized but extend out quite far relative to the other occupied (3p and 4s) orbitals. Indeed, the 3d orbitals tend to overlap with orbitals on neighboring atoms to form 3d conduction bands. Additionally, the 3d orbitals are vulnerable to crystal field interactions, V_{CF}, and any orbital polarization (OP) contribution to the total magnetic moment is largely quenched. Indirect relativistic effects act to enhance this effect. Any enhancement of orbital moments through the spin-orbit interaction, V_{SO} are expected to be minimal because the atomic number, Z, is relatively small in 3d transition metals. The crystal field interaction has much more influence than SO coupling in these systems. Consequently, the spin-magnetic moment is expected to be much larger than the orbital magnetic moment [41].

It follows that magnetic moments in Fe, Co, and Ni are expected to be described very well by LSDA alone. These systems can then be used to examine more refined corrections, such as SO and OP. Indeed, spin and orbital magnetic moments (Figs. (2) and (3), respectively) have been calculated [30, 41] for Fe, Co, and Ni with the spin-polarized relativistic

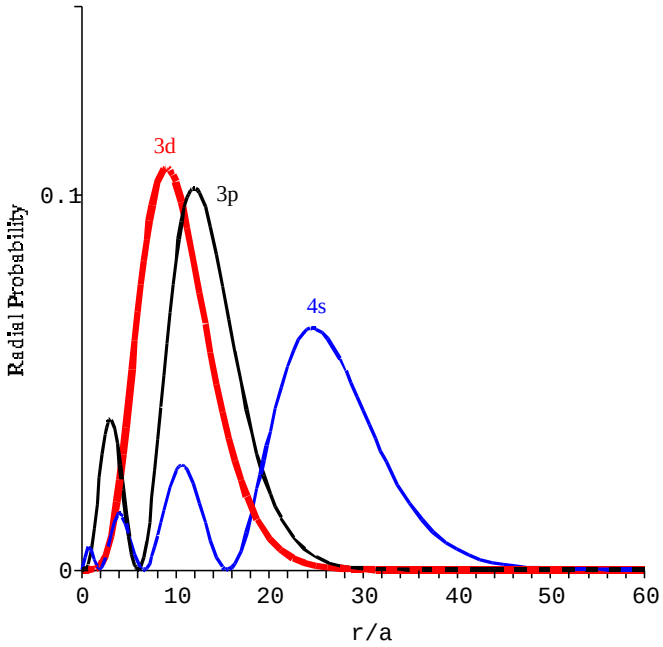

FIG. 1: Radial probability density of 3p, 3d, and 4s hydrogen electrons. The 3d electron density is largely localized, but has an extended tail exposed to crystal field interactions.

DFT(LSDA) scheme outlined in section (IIIA). The results are compared with values obtained from neutron scattering experiments [42]. The spin moment matches the experimental data very well. There is no affect of adding in SO and OP corrections to the spin moment calculation. This indicates that exchange-correlations contained within LSDA appear to be quite reasonable for these 3d metals. Of course, the orbital moments are zero within LSDA. By adding on a SO correction to the LSDA calculation, a small orbital moment is obtained, and better agreement is obtained with orbital moments measured by neutron scattering. Even better agreement with experiment is obtained when the orbital polarization correction is added into the calculation. Note that the spin and orbital moments have the same sign, in accordance with Hund's third rule for more than half filled shells. Based on the spin moments, one might have guessed that iron would have the largest orbital moment. This

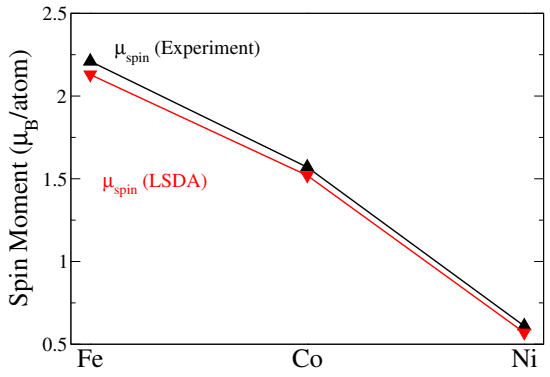

FIG. 2: Comparison of (LSDA) calculated [41] (down triangles) and experimental [42] (up triangles) spin moments for Fe (bcc), Co (hcp), and Ni (fcc). LSDA performs very well for spin moments in 3d systems.

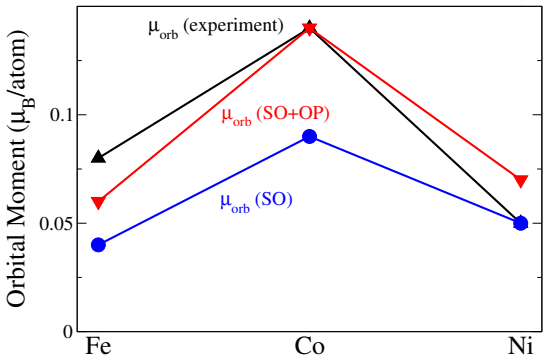

FIG. 3: Comparison of calculated [41] and experimental [42] (up triangles) orbital moments for Fe (bcc), Co (hcp), and Ni (fcc). Computed results including only a SO correction (circles) are plotted against results containing an additional OP correction (down triangles). This reveals the difference in magnitude of the SO-induced orbital moment relative to the total orbital moment in 3d systems. Best agreement with experiment is achieved when both corrections are applied.

is evidence that the different ground state crystal structures in Fe (bcc), Co (hcp), and Ni (fcc) have a significant effect on the relative magnitudes of crystal field quenching [41].

B. Lanthanides: ($V_{CF} \ll V_{SO}$)

Contrary to the 3d transition metals, the lanthanides are the archetypal localized magnetic systems [43]. Fig. (4) shows that the 4f orbital is much more spatially localized near the nucleus relative to the outer orbitals. In addition, Z is still small enough that indirect relativistic effects do not push the 4f orbital out much. In fact, the 4f orbitals do not extend out far enough to become bonding orbitals and, therefore, the 4f electrons tend to remain associated with their respective paramagnetic ions. This means that Hund's rules for the free atom still apply to these systems. Another consequence of the highly-localized 4f orbitals

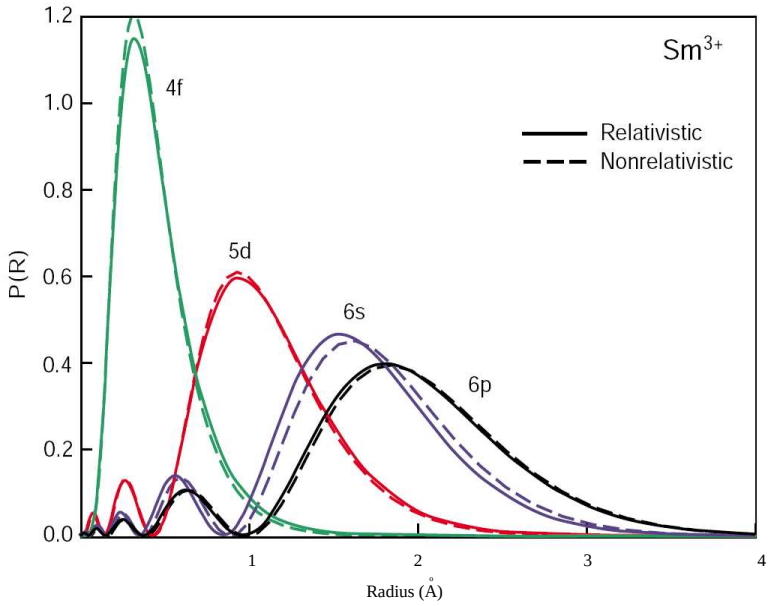

FIG. 4: Radial probability density of 4f, 5d, 6s, and 6p Sm^{3+} electrons. The 4f electron density is strongly localized near the nucleus and largely unaffected by crystal fields. The direct and indirect relativistic effects can been seen from the difference in the dashed and solid lines. Figure adapted from Ref. [45]

is that there is very little interaction with crystal fields. Therefore, the orbital moment is not quenched as it is in 3d systems. The 4f systems also have a much larger Z than 3d systems, and the spin-orbit interaction is expected to have much larger influence on magnetic moments than crystal fields. Indeed, very large orbital moments are expected in 4f systems [43, 44].

Consequently, *total* magnetic moments in 4f systems are not expected to be described well by LSDA alone. Fig. (5) shows the calculated spin orbital moments of Ce(fcc), Pr(fcc), and Nd(fcc) solids within spin-polarized relativistic DFT(LSDA). (There are currently no experiments for direct comparison of *spin* moments.) The large orbital moments expected in these systems are obtained by adding on SO [46] and OP [29] corrections, as shown in Fig. (6). Once again, the spin and orbital moments have opposite sign in accordance with Hund's third rule for less than half filled shells. It should be noted that the SO+OP orbital

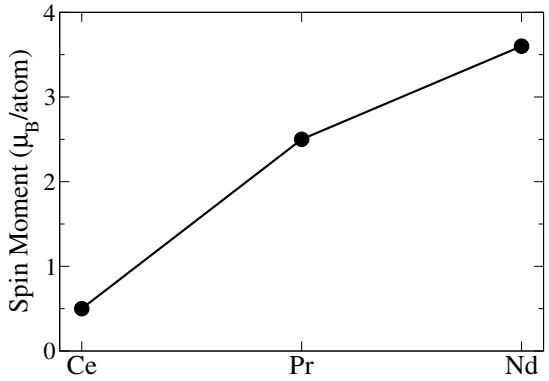

FIG. 5: Calculated [46] spin moments for Ce, Pr, and Nd within LSDA.

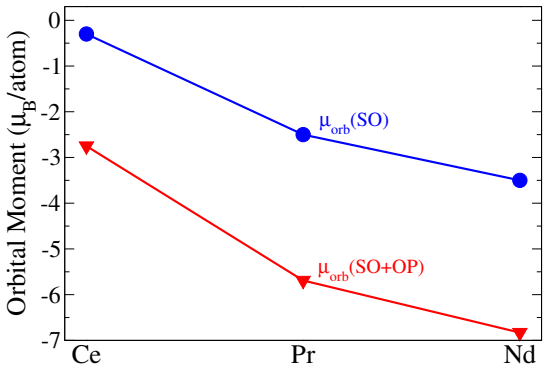

FIG. 6: Comparison of Ce, Pr, and Nd orbital moments: 1) Calculated with only the SO correction [46] (circles) and 2) Calculated with both SO and OP corrections (down triangles) [29].

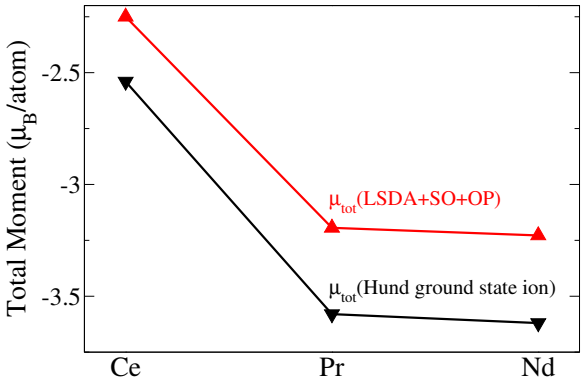

FIG. 7: Comparison of total moments for Ce, Pr, and Nd: 1) Using LSDA values which included SO, and OP corrections (up triangles) [29] and 2) The total moment predicted by Hund's rules for the free ions in their natural +3 oxidation state (down triangles). Hund's rules for the free ion are expected to apply to the localized 4f state, and are therefore a measure of the accuracy of the calculation.

moment is an estimated value that was calculated indirectly ($\mu_{orb} = \mu_{tot} - \mu_{spin}$) with Hund's rules (Eq. (4)) using LSDA values of S_z and L_z from Ref. [29]. The validity of doing this is shown by Fig. (7), which compares the calculated total moment (from S_z and L_z) for the solid compared with the values predicted by Hund's rules for the free ions. The reasonably close agreement between these two values indicates that Hund's rules still apply roughly to the localized 4f states.

C. Actinides: ($V_{CF} \simeq V_{SO}$)

The actinide (5f) elements are unique in that there is a change from itinerant to localized-electron behavior as one proceeds across the periodic table [47–50]. This behavior is suggested by considering a plot of atomic volumes for the 3d, 4f, and 5f elements as a function of electron count. Fig. (8) shows that the atomic volume of the light actinides (Th-Np) follows the parabolic decrease with increasing electron count that is observed in the 3d transition metals. This is an indication that each additional electron is going into the conduction band to participate in bonding, resulting in a decreased volume. At Pu, there is an abrupt increase in the actinide volume, and they behave more like 4f elements. The slight contraction visible for the 4f and heavy 5f elements indicates that electrons are being added to a localized, core state. The implication is that, light actinides follow an itinerant model of magnetism, while a localized model is more appropriate for heavy actinides.

Fig. (9) shows that the underlying mechanism behind this itinerant-localized behavior lies in the fact that, in the light actinides, the 5f orbitals are slightly more extended than the 4f orbitals (compare the probability at 1 Å, for example). Also, a close look at the relativistic density reveals that indirect relativistic effects have a larger effect on 5f electrons, increasing the radial extent of the 5f wave functions. This extra extension is enough to allow for the 5f orbitals to overlap with neighboring orbitals and become bonding orbitals by forming small conduction bands. Consequently, crystal fields will partially quench the angular momentum in these systems. However, there will be large spin-orbit effects due to the large Z-number, and a significant orbital moment can be induced. It is expected that the spin-orbit and crystal field interactions will be of similar order of magnitude, and, consequently, spin and orbital moments are of similar magnitude. In fact, for less than half filled shells, the spin and

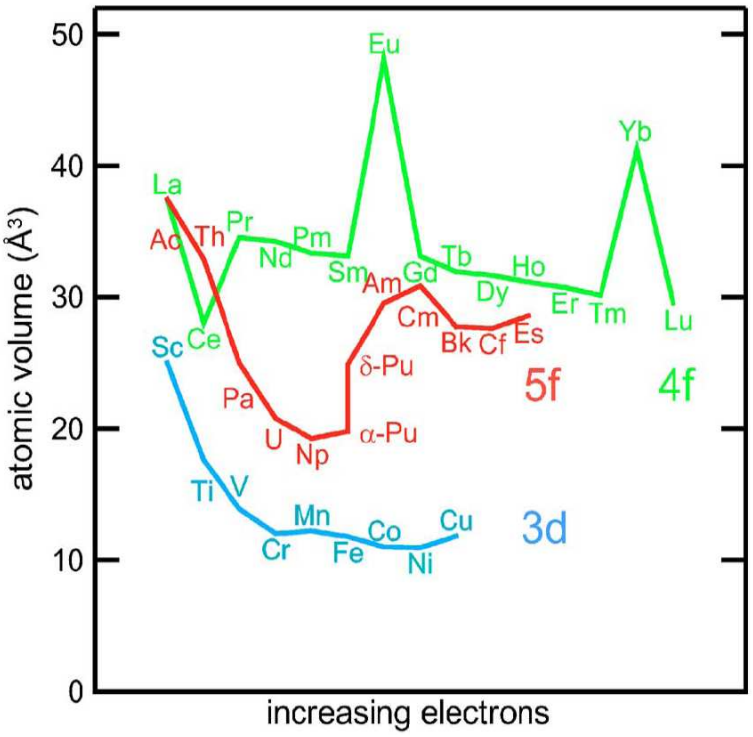

FIG. 8: Atomic volumes (equilibrium volume per atom in the primitive unit cell) of the 3d, 4f, and 5f elements as a function of the electron count, increasing to the right. The 5f elements follow the parabolic behavior of the 3d elements up to Pu. Then there is an abrupt change in volume, after which the 5f elements follow the 4f trend more closely. This demonstrates the switch from itinerant to localized behavior in the 5f row of elements. Figure taken from Ref. [45, 50]

orbital moments may exactly cancel [28, 34, 50–53]. Now, as one proceeds across the actinide row in the periodic table, the 5f orbitals contract as Z increases and the 5f orbitals become localized. In fact, at Bk, the 5f orbitals reach the same degree of localization observed in the lanthanides [49].

Measured and calculated moments of pure, light actinide metals are fairly scarce in the literature because those atoms tend to have no magnetic moment [49]. Data on heavy actinides is even more scarce since they do not exist in measurable quantities. However, laves-phase compounds, such as UFe_2, $NpFe_2$, and $PuFe_2$ are ferromagnetic below certain temperatures and have undergone a relatively extensive theoretical and experimental study.

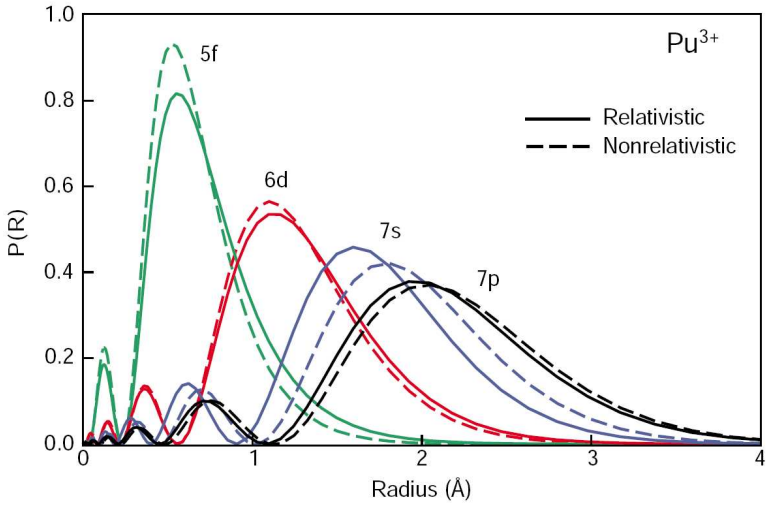

FIG. 9: Radial probability density of 5f, 6d, 7s, and 7p Pu^{3+} electrons. The 5f orbital in light actinides is localized, but more extended than the 4f orbitals in lanthanides. The 5f orbitals are also more vulnerable to crystal field effects (compare with 4f orbital at 1 Å, for example). In the heavy actinides (Am and beyond), the 5f orbitals are localized to a similar extent as 4f orbitals in lanthanides. Dashed and solid lines indicate direct and indirect relativistic effects. Figure adapted from Ref. [45]

To stay within the scope of this paper, focus will be placed on the magnetic moments of the 5f electrons in the actinide element and not on the interactions going on between the 5f and 3d elements.

The spin and orbital moments (Figs. (10) and (11), respectively) of the 5f electrons in UFe_2, $NpFe_2$, and $PuFe_2$ have been calculated within the spin-polarized relativistic DFT(LSDA) including both SO and OP corrections [54, 55]. The spin and orbital moments are in opposite directions in accordance with Hund's third rule and they are almost equal in magnitude for each element. The 5f spin moments are somewhat lower than experimental values. Compared with the 3d itinerant spin moment, the agreement is much worse. This is an indication that exchange correlation captured by LSDA may not be as sufficient in the 5f systems. The orbital moments calculated with SO and SO+OP are roughly in agreement with experiment. However, the results are puzzling in that the orbital moment calculated

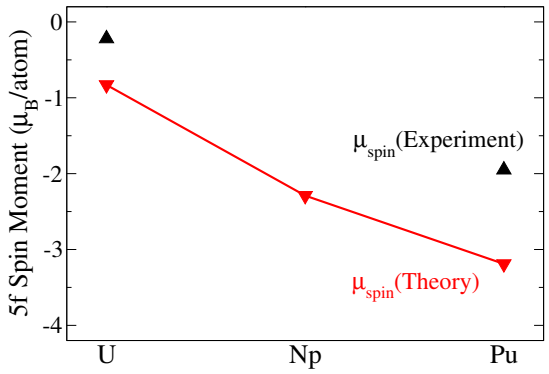

FIG. 10: Comparison of calculated [54, 55] (down triangles) and experimental [35] (up triangles) 5f spin moments for UFe_2, $NpFe_2$, $PuFe_2$ in the cubic laves-phase. Agreement with experiment is reasonably good, however error is large compared with 3d and 4f systems. (There is no experimental data for Np).

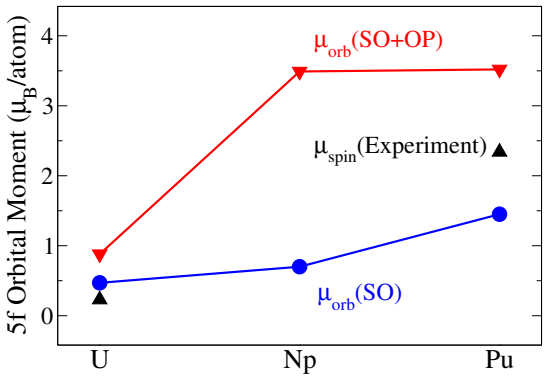

FIG. 11: Comparison of calculated [54, 55] and experimental [35] (up triangles) 5f orbital moments for UFe_2, $NpFe_2$, and $PuFe_2$ in the cubic laves-phase. Computed results including only a SO correction (circles) are plotted against results containing an additional OP correction (down triangles). Agreement with experiment is reasonably good for both calculations. However, in this case, adding in the OP correction appears to result in worse agreement with experiment. There is no experimental data for Np.

with the OP correction is in worse agreement in this case, lying higher than experiment. This could be interpreted as a sign of the ad-hoc OP correction breaking down. Finally, Fig. (12) shows that when the spin and orbital moments are added together, the total moment agrees extremely well with the neutron scattering measurement. At this point, there is no explanation for why a cancellation of errors leads to the total moments agreeing so well with experiment when the spin and orbital moments clearly do not.

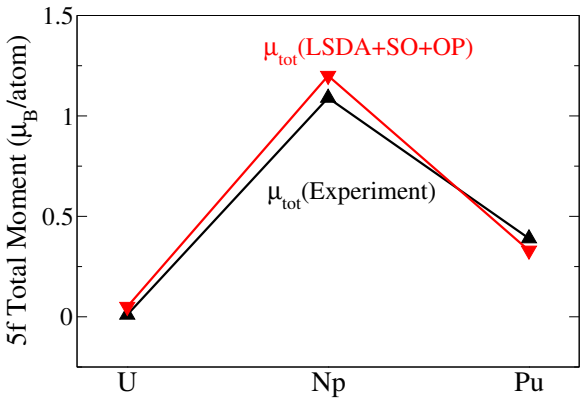

FIG. 12: Comparison of calculated (down triangles) and experimental [34–36, 53, 56] (up triangles) 5f total moments for UFe_2, $NpFe_2$, and $PuFe_2$ in the cubic Laves-phase. Calculated values include spin polarization, SO, and OP corrections. Even though the individual spin and orbital moments do not show perfect agreement with experiment (previous two figures), when they are summed, the total moment shows a drastic improvement in accuracy via (unexplained) cancellation of errors.

V. CONCLUSION

This paper has examined the role of relativity in magnetism and focused on calculating magnetic moments in solids. In particular, the theory of relativistic, spin-polarized DFT within the LSDA was reviewed and calculations of 3d, 4f, and 5f atomic magnetic moments using this method were compared with neutron scattering measurements. The importance of treating spin polarization, spin-orbit coupling, and orbital polarization was emphasized for obtaining both spin and orbital moments. The fact that calculations agreed well with experiment for transition metals and rare earths indicates that the spin-polarized DFT scheme used is flexible enough to handle both itinerant and localized systems. The main results were that pure LSDA describes 3d transition metals well due to the crystal field quenching of the orbital moment. However, there is a small orbital moment contribution induced by spin-orbit coupling. In the more localized 4f and 5f systems, LSDA alone is not adequate to calculate total magnetic moments that agree with experiment. The localized wave functions

reduce the amount of crystal field splitting, which significantly increases the orbital contribution to the total magnetic moment. The spin-orbit coupling is also increased relative to the transition metals due to the larger atomic numbers. Therefore in these systems, it is essential to make spin-orbit and orbital polarization corrections to LSDA. With experimental agreement being worse in the actinide systems, it was speculated that the LSDA and the *ad hoc* orbital polarization correction are not quite adequate for the 5f electrons. At least, these examples are certainly illustrative of the importance of relativistic effects in magnetism.

Acknowledgments

Thanks to my advisor, Prof. J. W. Wilkins, for providing an interesting topic and for the many useful discussions and suggestions. Much appreciation also goes to the support of my committee: Profs. A. Epstein, R. Furnstahl, and C. Jayaprakash. Additionally, I would like to acknowledge worthwhile discussions with Richard Hennig, and useful email correspondence with Olle Eriksson and Angus Lawson.

---

[1] R. Shankar, *Principles of Quantum Mechanics* (Kluwer Academic, New York, 1994), 2nd ed.

[2] J. D. Bjorken and S. D. Drell, *Relativistic Quantum Mechanics* (McGraw-Hill, New York, 1964).

[3] P. Novák, *Calculations of spin-orbit coupling*, `www.wien2k.at/reg_user/textbooks/` (2001).

[4] P. Pyykkö, Chem. Rev. **88**, 563 (1988).

[5] S. Blundell, *Magnetism in Condensed Matter* (Oxford University Press, New York, 2001).

[6] R. Tilley, *Understanding Solids: The Science of Materials* (John Wiley and Sons, Chichester, 2004).

[7] M. P. Marder, *Condensed Matter Physics* (John Wiley and Sons, New York, 2000).

[8] C. Kittel, *Introduction to Solid State Physics* (John Wiley and Sons, New York, 1996), 7th ed.

[9] N. W. Ashcroft and N. D. Mermin, *Soild State Physics* (Thomson Learning, USA, 1976).

[10] U. Kaldor, E. Eliav, and A. Landau, *Theoretical Chemistry and Physics of Heavy and Superheavy Elements* (Kluwer, Dordrecht, 2003), pg. 172.

[11] H. J. F. Jansen, Physics Today **48**, 50 (1995).

[12] P. Schwerdtfeger, ed., *Relativistic Electronic Structure Theory, Part 1: Fundamentals*, vol. 11 of *Theoretical and Computational Chemistry* (Elsevier, San Diego, 2004).

[13] S. Wilson, ed., *Relativistic Effects in Atoms and Molecules*, vol. 2 (Plenum, New York, 1987).

[14] P. Hohenberg and W. Kohn, Phys. Rev. **136** (1964).

[15] W. K. L. J. Sham, Phys. Rev. **140** (1965).

[16] P. Strange, *Relativistic Quantum Mechanics: with applications in condensed matter and atomic physics* (Cambridge University Press, Cambridge, 1998).

[17] D. Ceperley and B. J. Alder, Phys. Rev. Lett. **45**, 566 (1980).

[18] A. K. Rajagopal and J. Callaway, Phys. Rev. B **7**, 1912 (1973).

[19] M. V. Ramana and A. K. Rajagopal, Adv. Chem. Phys. **54**, 231 (1983).

[20] E. Engle, R. M. Dreizler, S. Varga, and B. Fricke, *Relativistic Effects in Heavy-Element Chemisty and Physics* (Wiley, Chichester, 2003).

[21] B. L. Gyorffy, J. B. Staunton, H. Ebert, P. Strange, and B. Ginatempo, *The Effects of Relativity in Atoms, Molecules, and the Solid State.* (Plenum, New York, 1991).

[22] L. Nordström, Ph.D. thesis, Uppsala (1991).

[23] A. H. MacDonald and S. H. Vosko, J. Phys. C: Solid State Phys. **12**, 2977 (1979).

[24] W. Gordon, Z. Phys **50**, 630 (1928).

[25] U. V. Barth and L. Hedin, J. Phys. C: Solid State Phys. **5**, 1629 (1972).

[26] D. J. Singh and L. Nordström, eds., *Planewaves, Pseudopotentials, and the LAPW Method* (Springer, 2006), 2nd ed.

[27] M. Richter, J. Phys. D: Appl. Phys. **31**, 1017 (1998).

[28] M. S. S. Brooks and P. J. Kelly, Phys. Rev. Lett. **51**, 1708 (1983).

[29] O. Eriksson, M. S. S. Brooks, and B. Johansson, Phys. Rev. B **41**, 7311 (1990).

[30] O. Eriksson, L. Nordström, A. Pohl, L. Severin, A. M. Boring, and B. Johansson, Phys. Rev. B **41**, 11807 (1990).

[31] H. Eschrig, M. Richter, and I. Opahle, *Relativistic Electronic Structure Theory, Part 2: Ap-*

plications, vol. 14 of *Theoretical and Computational Chemistry* (Elsevier, San Diego, 2004).

[32] W. Marshall and S. W. Lovesey, *Theory of Thermal Neutron Scattering* (Oxford University, London, 1971).

[33] G. H. Lander, M. S. S. Brooks, and B. Johansson, Phys. Rev. B **43**, 13672 (1991).

[34] M. Wulff, G. H. Lander, J. Rebizant, J. C. Spirlet, B. Lebech, and C. Broholm, Phys. Rev. B **37**, 5577 (1988).

[35] B. Lebech, M. Wulff, and G. H. Lander, J. Appl. Phys. **69**, 5891 (1991).

[36] M. Wulff, B. Lebech, A. Delapalme, G. H. Lander, J. Rebizant, and J. C. Spirlet, Physica B **156**, 836 (1989).

[37] J. Rossat-Mignod, G. H. Lander, and P. Burlet, *Handbook on the Physics and Chemistry of the Actinides* (North-holland, Amsterdam, 1984), vol. 1, chap. 6.

[38] J. P. Desclaux and A. J. Freeman, J. Magn. Magn. Mater. **8**, 126 (1978).

[39] W. Marshall and S. W. Lovesey, *Theory of Thermal Neutron Scattering* (Oxford University, London, 1971), pg. 152.

[40] E. P. Wohlfarth, ed., *Ferromagnetic Materials* (North-Holland, Amsterdam, 1980), vol. 1, chap. 1.

[41] O. Eriksson, B. Johansson, R. C. Albers, A. M. Boring, and M. S. S. Brooks, Phys. Rev. B **42**, 2707 (1990).

[42] M. B. Stearns, *Lamdolt-Börnstein Numerical Data and Functional Relationships in Science and Technology*, vol. 19, group 3, part a (Springer-Verlag, Berlin, 1986).

[43] R. Elliott, ed., *Magnetic Properties of Rare Earth Metals* (Plenum, New York, 1972).

[44] H. Drulis and M. Drulis, *Lamdolt-Börnstein Numerical Data and Functional Relationships in Science and Technology*, vol. 19, group 3, part d1 (Springer-Verlag, Berlin, 1986).

[45] S. S. Hecker, Los Alamos Science **No. 26**, 290 (2000).

[46] B. I. Min and Y. R. Yang, J. Phys.:Condens. Matter **3**, 5131 (1991).

[47] M. S. S. Brooks, B. Johansson, and H. L. Skriver, *Handbook on the Physics and Chemistry of the Actinides* (North-holland, Amsterdam, 1984), vol. 1, chap. 3.

[48] A. J. Arko, D. D. Koelling, and J. E. Schirber, *Handbook on the Physics and Chemistry of the Actinides* (North-holland, Amsterdam, 1984), vol. 2, chap. 3.

[49] S. Troć, *Lamdolt-Börnstein Numerical Data and Functional Relationships in Science and Tech-*

nology, vol. 19, group 3, part f1 (Springer-Verlag, Berlin, 1986).

[50] J. C. Lashley, A. Lawson, R. J. McQueeney, and G. H. Lander, Phys. Rev. B **72**, 54416 (2005).

[51] B. Johansson, O. eriksson, L. Nordström, L. Severin, and M. S. S. Brooks, Physica B **172**, 101 (1991).

[52] J. M. Fournier, P. Frings, M. Bonnet, J. X. Bouscherle, A. Delapalme, A. Menovsky, and J. Less, J. Less Common Metals **121**, 249 (1986).

[53] M. Wulff, G. H. Lander, B. Lebech, and A. Delapalme, Phys. Rev. B **39**, 4719 (1989).

[54] O. Eriksson, M. S. S. Brooks, and B. Johansson, Phys. Rev. B **41**, 9087 (1990).

[55] O. Eriksson, M. S. S. Brooks, B. Johansson, and R. C. Albers, J. Appl. Phys. **69**, 5897 (1991).

[56] G. H. Lander, A. T. Aldred, B. D. Dunlap, and G. K. Shenoy, Physica B **86-88**, 152 (1977).